Submillimeter Guided-Wave Experiments with Dielectric Rib Waveguides

MIKIO TSUJI, STUDENT MEMBER, IEEE, SHIGEFUMI SUHARA, HIROSHI SHIGESAWA, MEMBER, IEEE, AND KEI TAKIYAMA, MEMBER, IEEE

Abstract—**The transmission characteristics of rib waveguides are examined in the submillimeter-wave region at $\lambda_0 = 337$ μm. A number of miniature polyethylene rib waveguides are fabricated by means of a die-cast technique. The mode launching into such a waveguide is performed by focusing a laser beam directly on the end face of the waveguide, while the transmitted power is detected at any point on a waveguide through a movable grating coupler which can couple selectively with one of propagating modes. The measured phase constants show good agreement with the theoretical ones calculated by our analytical method, while the attenuation constants, typically $\alpha\lambda_0 = 4.5\times10^{-3}$ Np are found to be about 1.8 times as much as theoretical ones. Finally, the good confinement of fields in the rib portion is proved by means of two simple methods.**

I. INTRODUCTION

AT THE submillimeter-wave region, it is well known that many of the solid dielectric materials show a considerable absorption loss and only a few nonpolar polymers show a somewhat low absorptions. They are polyethylene (typical absorption coefficient at $\lambda_0 = 337$ μm $\alpha_a = 0.1$ Np/cm), polypropylene ($\alpha_a = 0.14$ Np/cm), and TPX (poly-4-methylpentene-1 : $\alpha_a = 0.16$ Np/cm) [1]. However, all of these polymers have almost the same refractive indexes (around 1.5), so that it is inevitable to construct a three-dimensional dielectric waveguide for use in submillimeter-wave integrated circuits with a single dielectric material instead of an effective combination of several kinds of low-loss materials having different refractive indices as seen in sophisticated waveguides in both millimeter-wave [2], [3], and optical frequencies [4], [5]. This is of particular requisite to a waveguide technique in the submillimeter-wave region, at least for the present.

One example of single material waveguides is the rib waveguide [6], as shown in Fig. 1. The purpose of this paper is to survey experimentally the transmission characteristics of polyethylene rib waveguides in the submillimeter-wave region at $\lambda_0 = 337$ μm. The techniques developed in the submillimeter-wave experiments of slab waveguides [7] will be used again successfully in the present experiments. When such experimental results should be discussed from the analytical point of view, we will meet considerable difficulty in obtaining an exact analysis because of its nonuniform boundary. Therefore, a simple analytical method, i.e., the approximate mode matching method [8] has been proposed and its usefulness has been proved through a number of millimeter-wave (50-GHz region) experiments [9]. This method will be also followed here.

Manuscript received September 30, 1980; revised December 17, 1980.

M. Tsuji, H. Shigesawa, and K. Takiyama are with the Department of Electronics, Doshisha University, Kyoto, 602 Japan.

S. Suhara was with the Department of Electronics, Doshisha University, Kyoto, Japan. He is now with the Sanyo Electric Company, Osaka, 573 Japan.

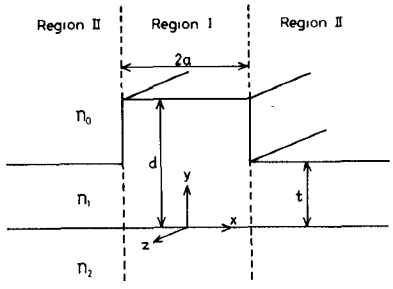

Fig. 1. Cross section of a rib waveguide.

II. ANALYSIS

Fig. 1 shows the geometry of a dielectric rib waveguide. As expected in this waveguide, all the modes are indeed hybrid in the rigorous sense. In a rough approximation, however, there may be TE and TM waves with respect to the y direction [10] and approximate analyses [11]–[14] assume often the presence of only one type of these waves as a characteristics mode as in a dielectric rectangular waveguide [4]. One type, which we call the TE_y mode, is polarized predominantly in the x direction and has $E_y = 0$, while the other mode, TM_y, is polarized predominantly in the y direction and has $H_y = 0$. For the present, let us direct our attention to the TE_y modes.

Now, let us subdivide the cross section of this guide into two constituent regions, i.e., regions I and II, and consider separately each of those regions, as if the region I is a rectangular dielectric waveguide and region II is semiinfinite slab waveguide. We assume that all the field components can be expanded into the propagating surface modes with unknown modal amplitudes A_m and B_m in each region similar to [15].

Considering the energy concentration in the rib portion, the E_x components in each region can be expressed for the TE_y modes as follows:

$$E_x^{\mathrm{I}} = \sum_m A_m f_m^{\mathrm{I}}(y)\cos(\kappa_m x + \varphi)\exp j(\omega t - hz), \quad \text{for region I} \quad (1)$$

$$E_x^{II}=\sum_m B_m f_m^{II}(y)\exp(-\delta_m|x-a|)\exp j(\omega t-hz),$$

for region II (2)

where h denotes the phase constant to be found and φ is a parameter to express the symmetry of fields with respect to the y–z plane at $x=0$. The functions f_m^I and f_m^{II} are the variations in the y direction which are described as

$$f_m^I(y)=\begin{cases}\sin(\beta_m^I d+\phi_m^I)\exp\{-\alpha_m^I(y-d)\}, & y\geqslant d\\ \sin(\beta_m^I y+\phi_m^I), & 0\leqslant y\leqslant d\\ \sin\phi_m^I\exp(\gamma_m^I y), & y\leqslant 0\end{cases} \tag{3}$$

$$f_m^{II}(y)=\begin{cases}\sin(\beta_m^{II} t+\phi_m^{II})\exp\{-\alpha_m^{II}(y-t)\}, & y\geqslant t\\ \sin(\beta_m^{II} y+\phi_m^{II}), & 0\leqslant y\leqslant t\\ \sin\phi_m^{II}\exp(\gamma_m^{II} y), & y\leqslant 0\end{cases} \tag{4}$$

with the conservation relations of wavenumbers

$$(n_1^2-n_0^2)k_0^2=(\alpha_m^I)^2+(\beta_m^I)^2=(\alpha_m^{II})^2+(\beta_m^{II})^2 \tag{5}$$

$$(n_1^2-n_2^2)k_0^2=(\gamma_m^I)^2+(\beta_m^I)^2=(\gamma_m^{II})^2+(\beta_m^{II})^2 \tag{6}$$

and the phase constant h is given by

$$h^2=(n_1k_0)^2-(\beta_m^I)^2-(\kappa_m)^2=(n_1k_0)^2-(\beta_m^{II})^2+(\delta_m)^2. \tag{7}$$

The other components of wave fields can be derived from the following equations:

$$H_x=\frac{1}{\omega\mu h}\frac{\partial^2}{\partial x\partial y}E_x$$

$$H_y=\frac{1}{\omega\mu h}\left(\frac{\partial^2}{\partial x^2}-h^2\right)E_x,\qquad E_y=0$$

$$H_z=-\frac{j}{\omega\mu}\frac{\partial}{\partial y}E_x,\qquad E_z=-\frac{j}{h}\frac{\partial}{\partial x}E_x. \tag{8}$$

First, let us determine these fields in each region so as to fulfill the boundary conditions on the core-substrate boundary at $y=0$ and on the x–z plane at $y=d$ in the region I or at $y=t$ in the region II. As a result, it is easily found that the wavenumbers $j\alpha_m$, β_m, and $j\gamma_m$ in the y direction can be obtained independently of those in the x direction from the following well-known eigenvalue equations of asymmetric slab waveguide:

$$\tan\beta_m^I d=\beta_m^I(\alpha_m^I+\gamma_m^I)/(\beta_m^{I2}-\alpha_m^I\gamma_m^I) \tag{9}$$

$$\tan\beta_m^{II} t=\beta_m^{II}(\alpha_m^{II}+\gamma_m^{II})/(\beta_m^{II2}-\alpha_m^{II}\gamma_m^{II}). \tag{10}$$

Thus the parameters α_m, β_m, γ_m, and ϕ_m should be recognized hereafter as the known ones.

Next, we must impose the continuity condition of the tangential fields through the infinite y–z plane at $x=a$, i.e., $\mathbb{A}_x\times(\mathbb{E}^I-\mathbb{E}^{II})=0$ and $\mathbb{A}_x\times(\mathbb{H}^I-\mathbb{H}^{II})=0$, where $\mathbb{A}_x$ is the unit normal vector to this plane. However, the approximate fields presented here do not necessarily satisfy this type of boundary condition, so that let us fit the fields to this boundary condition in the sense of least-squares [14], [16]. For this purpose, let us introduce the mean-squares error F defined by the following equation:

$$F=\int_{-\infty}^{\infty}|\mathbb{A}_x\times(\mathbb{E}^I-\mathbb{E}^{II})|_{x=a}^2\,dy+\left(\frac{\omega\mu}{n_\nu k_0}\right)^2\int_{-\infty}^{\infty}|\mathbb{A}_x\times(\mathbb{H}^I-\mathbb{H}^{II})|_{x=a}^2\,dy \tag{11}$$

where n_ν means n_0, n_1, and n_2.

If the thickness d and t are such that only a single surface wave mode can be supported on each region, it is reasonable to consider the single-mode approximation, in which only a fundamental mode of $m=0$ in (1) and (2) are taken into account. In this case, the unknown variables to be solved become A_0, B_0, and h at the chosen frequency ω. But, we have a freedom to define arbitrarily one of two expansion coefficients, so that by setting $B_0=1$, the quantity F can be expressed as follows:

$$F(A_0,h,\omega)=A_0A_0^*P(h,\omega)+A_0Q(h,\omega)+A_0^*Q^*(h,\omega)+R(h,\omega) \tag{12}$$

where the symbol $*$ denotes the complex conjugate and P, Q, R are the functions of the phase constant h and the frequency ω, of which explicit but tedious forms can be found in [9, appendix].

After introducing the mode matching procedure in which the quantity F should be minimized with respect to A_0^*, the variational method to F derives the minimum value $\tilde{F}$ of F as follows:

$$\tilde{F}(h,\omega)=R(h,\omega)-|Q(h,\omega)|^2/P(h,\omega). \tag{13}$$

Finally, the dispersion curve of the guided mode can be calculated through the relation of $\partial\tilde{F}(h,\omega)/\partial h=0$. Practically, it is easy to find out numerically h at which the quantity $\tilde{F}$ takes the minimum value for a fixed frequency ω.

Once the phase constant is found, the field distributions (or eigenfunctions) can be easily obtained by substituting B_0 $(=1)$ and A_0 found by the mode matching procedure into (1), (2) and so on. Then the perturbation technique may be utilized to calculate the attenuation characteristics of a rib waveguide.

On the other hand, we know another single-mode approximation called as the effective dielectric constant (EDC) method [13]. This method replaces each region of Fig. 1 with an infinite homogeneous region in the y direction having some effective dielectric constant, and such a hypothetical structure is used to match the tangential fields on the boundaries, and the propagation constant is determined. The EDC method gives indeed a good approxi-

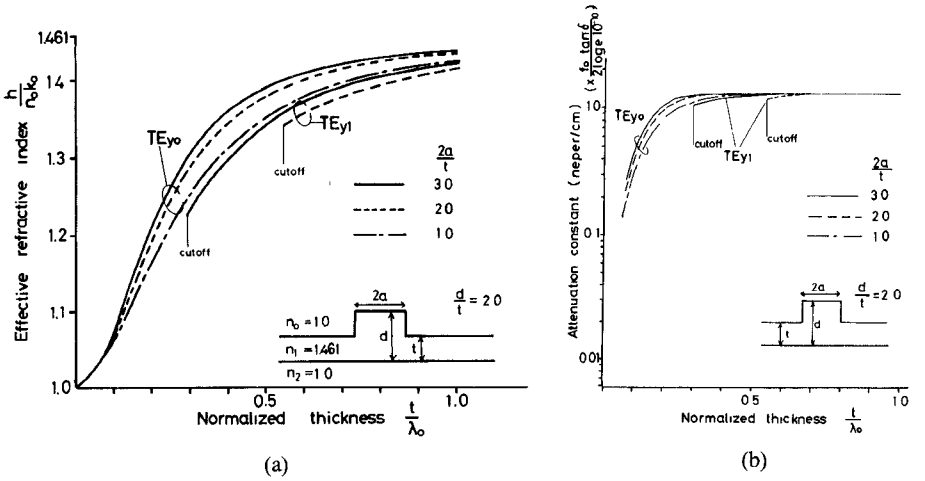

Fig. 2. Propagation characteristics for the TE_y mode with a thickness ratio $d/t=2.0$. (a) Phase constant. (b) Attenuation constant.

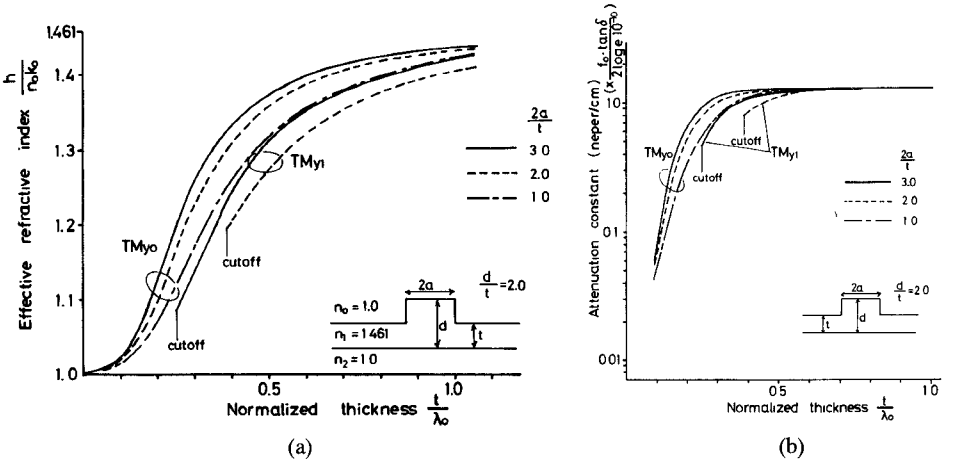

Fig. 3. Propagation characteristics for the TM_y mode with a thickness ratio $d/t=2.0$. (a) Phase constant. (b) Attenuation constant.

mation for the propagation constant as discussed in [9] by comparison with other methods. However, this method is not reliable for the field distribution by the reason mentioned previously, and may be not effective to calculate the transmission loss.

Now, in our experiments, the refractive indices n_0 and n_2 indicated in Fig. 1 are assumed to be real and unity (air) and the dielectric material of a guide is assumed to be a polyethylene of which refractive index n_1 is less sensitive to the submillimeter-wave frequencies and is almost kept on about $n_1=1.46$.

Consequently, the typical calculated results of the phase constant h and the attenuation constant α for each propagating modes are shown in Figs. 2 and 3, where the effective refractive index h/n_0k_0 and the attenuation constant normalized by both $\tan\delta$ and the frequency f_0 (in H_z) are employed instead of h and α themselves, respectively. The TE_{y1} (or TM_{y1}) mode in these figures means the next higher order mode which has an antisymmetric E_x (or H_x) component with respect to the y–z plane at $x=0$.

III. Experiments

A. Experimental Setup

By referring the theoretical results, several kinds of rib waveguide having different t, d, and a were made of commercial polyethylene powders by means of a die-cast technique. Each waveguide has the lateral width of 30 mm and the propagation length of 250 mm.

Now, the key point of our accurate and reliable techniques developed for the submillimeter-wave experiments [7], [17] is the employment of the movable grating coupler which can couple selectively with one of the propagating modes and is movable along the guide surface, keeping up a constant coupling efficiency.

The experimental setup of Fig. 4 is similar to that employed in [9], where a rib waveguide is held tightly on a metal frame as shown in Fig. 5. Now, the laser beam from an HCN laser is split into two beams with a beam splitter made of a polyethylene film and one of them is led to a Golay cell detector for monitoring the output power of the

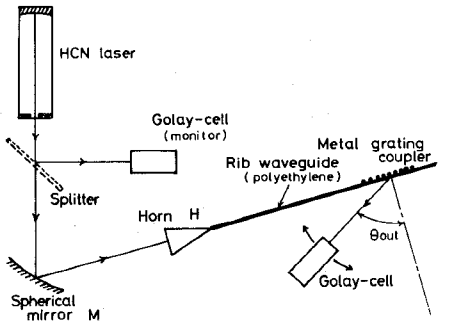

Fig. 4. Schematic diagram of the experimental setup.

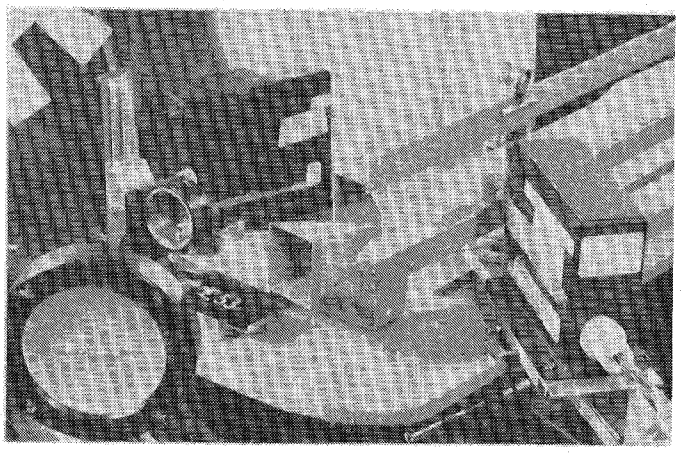

Fig. 5. External view of the experimental setup.

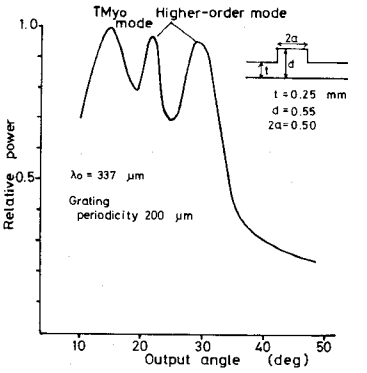

Fig. 6. Relative output powers radiated from the metal grating coupler as a function of the output angle.

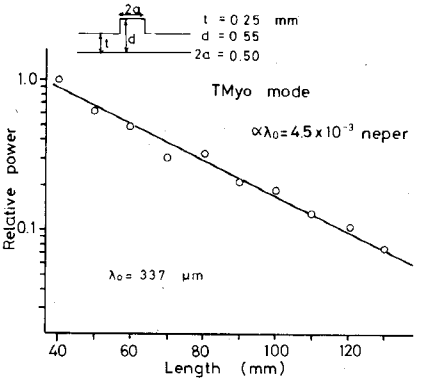

Fig. 7. Loss measurement for the TM_{y0} mode.

laser, while the other beam with a horizontal or a vertical polarization is launched into a rib waveguide to excite the TM_y or TE_y modes after focusing the beam on the end face of a rib portion through a spherical mirror and a metal horn.

On the other hand, a movable grating coupler which is made of Molybdenum wires of 100 μm in diameter arranged with a period of 200 μm over 15-mm length (75 periods) are mechanically contacted on the waveguide surface (the reverse side of a rib) so as to couple with a fraction of the transmitted power. The direction θ_{out} of a radiated beam from the coupler is measured with another Golay cell detector mounted on the rotatable arm around the coupler as seen from Figs. 4 and 5. Such a radiation angle makes it possible to obtain the phase constant of each propagating mode through the phase matching condition of a grating coupler (e.g., (1) of [7]).

Moreover, the attenuation constant of each propagation mode can be easily found by measuring the relative output power from the coupler as a function of the transmission length between the mode launcher and the coupler.

B. Phase and Attenuation Constants

Since the TE_y modes have a predominant electric field parallel to the metal wires of a grating, it is hard to couple efficiently with TE_y modes. Thus the experiments described here will examine the characteristics of TM_y modes only.

A typical example for the radiation intensity from a grating coupler is shown in Fig. 6 as a function of the output angle θ_{out}. We can observe clearly three peaks at around $\theta_{out}=15°$, 21°, and 28°. Theoretically, the θ_{out} of the TM_{y0} mode is found to be 15.7°. Moreover, if the launched beam is not trapped around the rib portion, but propagates in the form of the fundamental TM mode in a slab waveguide with a thickness t, we can find the radiation angle for such a mode to be 19.5°. These facts will allow us to conclude that the first peak at around 15° corresponds right to the TM_{y0} mode. The deviation between angles obtained theoretically (15.7°) and experimentally (15°) means the difference of about 0.8 percent in terms of the phase constant.

On the other hand, Fig. 7 shows an example of relative output powers from the coupler. Since the measured data have only a little fluctuation from a straight line, we may trust the sufficient accuracy of our loss measurements, and this result gives the measured attenuation constant at $\lambda_0 = 337$ μm as $\alpha\lambda_0 = 4.5\times10^{-3}$ Np which is about 1.8 times as much as the theoretical value obtained in the preceding section.

It is well known that the loss tangent $\tan\delta$ of a polyethylene follows the experimental curve given by the following equation [18]:

$$\tan\delta=\left(0.85+0.15\times10^{-4}/\lambda_0\right)\times10^{-4} \qquad (14)$$

where the wavelength λ_0 should be entered in micrometers (μm) and which is available in the limited bounds of 200 $\mu m<\lambda_0<1000$ μm. This relation brings about the $\tan\delta$ at

TABLE I
MEASURED AND THEORETICAL VALUES OF BOTH THE PHASE AND ATTENUATION CONSTANTS FOR THE TM_{y0} MODE

NO	Dimension			Measured values			Theoretical values		
	t (mm)	d (mm)	2a (mm)	Output angle θ_{out}(deg)	Phase constant h/n_0k_0	Attenuation constant (neper/cm)	Output angle θ_{out}(deg)	Phase constant h/n_0k_0	Attenuation constant (neper/cm)
1	0.20	0.45	1.00	1.5	1.42	144×10^{-3}	1.57	1.414	71.7×10^{-3}
2	0.11	0.18	0.70	2.5	1.26	93×10^{-3}	2.47	1.267	62.4×10^{-3}
3	0.25	0.55	0.50	1.5	1.42	134×10^{-3}	1.57	1.414	71.7×10^{-3}
4	0.12	0.33	0.50	1.8	1.37	112×10^{-3}	1.85	1.368	70.0×10^{-3}
5	0.15	0.35	0.40	1.8	1.37	128×10^{-3}	1.86	1.366	69.5×10^{-3}
6	0.15	0.26	0.30	2.2	1.31	120×10^{-3}	2.17	1.315	69.1×10^{-3}
7	0.10	0.21	0.30	2.5	1.26	98×10^{-3}	2.48	1.266	64.5×10^{-3}
8	0.08	0.19	0.30	2.6	1.25	91×10^{-3}	2.64	1.240	61.0×10^{-3}

$\lambda_0 = 337$ μm as 5.3×10^{-4} which is employed for the loss calculations throughout this paper.

However, the loss tangent of commercial polyethylene varies widely due to the presence of various additives, and it may be reasonable to consider that (14) gives the underestimated values for the actual polyethylene in our experiments. We have recently measured dielectric constants for polyethylene at $\lambda_0 = 337$ μm and have typically obtained $\tan\delta = 1.1\times10^{-3}$. See details in [22].

Now, the measured and calculated values for the TM_{y0} mode are summarized in Table I. It is clear from this table that the measured phase constants (i.e., output angle θ_{out}) show fairly good agreement with the theoretical ones calculated by our approximate method, while the attenuation constants are found to be about 1.8 times as much as theoretical ones. However, there are several modes in the experimental waveguide, and so most of the transmitting power of the TM_{y0} mode will be concentrated in the dielectric medium. This fact suggests that the attenuation constant will appear on the saturation region shown in Figs. 2(b) or 3(b).

By the way, the higher order modes indicated by the angles $\theta_{out} \simeq 21°$ and 28° at the second and third peaks in Fig. 6 show the measured attenuation constants of $\alpha\lambda_0 = 4.1\times10^{-3}$ Np and 3.3×10^{-3} Np, respectively. Such low attenuations will be due to less concentration of transmitting power in a waveguide. Thus it is interesting and useful for us to examine the attenuation characteristics of the single TM_{y0} mode with a thinner thickness by which it is expected to improve the loss characteristics.

C. Field Confinement in the Transverse Direction

In the submillimeter-wave region, it is truly impossible to measure the precise field distribution of a mode by means of a field probe which is commonly used in the microwave [19] and millimeter-wave [9], [20] regions. Then the field confinement in the transverse direction (the x direction of Fig. 1) is examined in comparison with a slab waveguide with a thickness t. For measuring the transverse broadening of the field, two simple methods described in [7] are again employed.

In the first method, the output power from a coupler is measured when a small absorber (3 mm^2 in area) is put on the surface of a guide and is moved along the transverse direction. Fig. 8(a) shows the results for a rib waveguide

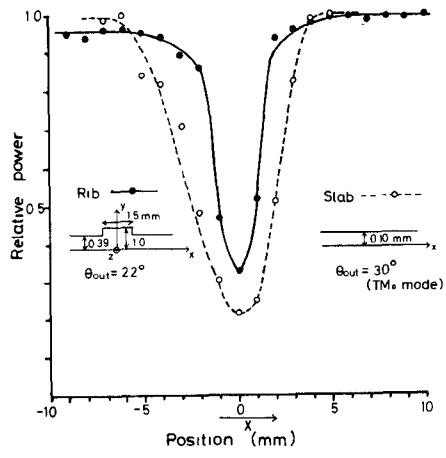

(a)

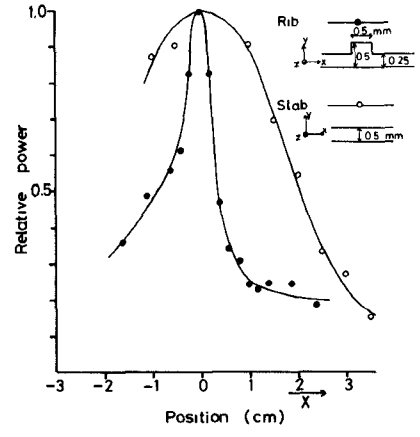

(b)

Fig. 8. Measurements of the transverse broadening of the field in the rib and slab waveguides. (a) Output powers are measured when a small absorber is moved on the surface of a waveguide. (b) Intensity distributions of the near field radiated from the end of a waveguide are measured by scanning a detector.

($t = 0.39$ mm, $d = 1.00$ mm, and $2a = 1.50$ mm) and a slab waveguide ($t = 0.10$ mm). It is clear from these results that the field is well confined in the rib portion.

In the second method, the near field patten of radiation from the end of a waveguide is measured by scanning the Golay cell detector along the transverse direction. The length of a guide is 130 mm and the near field pattern is measured at the distance of 70 mm apart from the end of a guide. The results shown in Fig. 8(b) indicate again the good confinement of field in a rib waveguide.

Such a good confinement of field in the transverse direction also proves that the metal frame holding a rib waveguide has no effects on the measurement of the attenuation constants.

IV. CONCLUSION

The phase and attenuation constants of polyethylene rib waveguides are measured in the submillimeter-wave region. As an example, the measured attenuation constant for the TM_{y0} mode in the multimode waveguide is $\alpha\lambda_0 = 4.5\times10^{-3}$ Np at $\lambda_0 = 337$ μm which is about 1.8 times as much as theoretical one when the loss tangent of a polyethylene

is assumed to be 5.3×10^{-4}. Now we are planning to examine the properties of a single mode guide. Moreover, in order to realize a low-loss guide, it will be necessary to introduce a technique which can reduce the absorption coefficient of a polyethylene [21]. These problems will be discussed in the following papers.

References

[1] G. W. Chantry, *Submillimeter Spectroscopy*. New York: Academic, 1971.

[2] R. M. Knox, "Dielectric waveguide microwave integrated circuits—An overview," *IEEE Trans. Microwave Theory Tech.*, vol. MTT-24, pp. 806–814, Nov. 1976.

[3] T. Itoh, "Inverted strip dielectric waveguide for millimeter-wave integrated circuits," *IEEE Trans. Microwave Theory Tech.*, vol. MTT-24, pp. 821–827, Nov. 1976.

[4] E. A. J. Marcatili, "Dielectric rectangular waveguide and directional coupler for integrated optics," *Bell Syst. Tech. J.*, vol. 48, pp. 2079–2102, Sept. 1969.

[5] R. M. Knox and P. P. Toulios, "Integrated circuits for the millimeter through optical frequency range," in *Proc. Symp. Submillimeter Waves*, (New York), Apr. 1970.

[6] J. E. Goell, "Rib waveguide for integrated optical circuits," *Appl. Opt.*, vol. 12, pp. 2797–2798, Dec. 1973.

[7] M. Tsuji, K. Kawai, H. Shigesawa, and K. Takiyama, "Submillimeter guided-wave experiments with polyethylene slab waveguides," *IEEE Trans. Microwave Theory Tech.*, vol. MTT-27, pp. 873–878, Nov. 1979.

[8] H. Shigesawa, M. Tsuji, S. Suhara, and K. Takiyama, "Approximated boundary value problem in a rib waveguide," URSI National Radio Science Meeting, Boulder, CO, B-5, Nov. 1979.

[9] M. Tsuji, H Shigesawa, and K. Takiyama, "Characteristics of dielectric rib waveguide analyzed by the approximated mode-matching method and its experiments in the millimeter wave region," *Trans. IECE Japan*, vol. 63B, pp. 884–891, Sept. 1980.

[10] R. F. Harrington, *Time Harmonic Electronic Fields*. New York: McGraw-Hill, 1961.

[11] V. Ramaswamy, "Strip-loaded film waveguide,' Bell Syst. Tech. J., vol. 53, pp. 697–704, Apr. 1974.

[12] H. Furuta, H. Noda, and A. Ihaya, "Novel optical waveguide for integrated optics," *Appl. Opt.*, vol. 13, pp. 322–326, Feb. 1974.

[13] W. V. McLevige, T. Itoh, and R. Mittra, "New waveguide structure for millimeter-wave and optical integrated circuits," *IEEE Trans. Microwave Theory Tech.*, vol. MTT-23, pp. 788–794, Oct. 1975.

[14] K. Yasuura, K. Shimohara, and T. Miyamoto, "Numerical analysis of a thin-film waveguide by mode-matching method," *J. Opt. Soc. Amer.*, vol. 70, pp. 183–191, Feb. 1980.

[15] R. Mittra, Y. L. Hou, and V. Jamnejad, "Analysis of open dielectric waveguides using mode-matching technique and variational methods," *IEEE Trans. Microwave Theory Tech.*, vol. MTT-28, pp. 36–43, Jan. 1980.

[16] K. Solbach and I. Wolff, "The electromagnetic fields and the phase constants of dielectric image lines," *IEEE Trans. Microwave Theory Tech.*, vol. 26, pp. 266–274, Apr. 1978.

[17] M. Tsuji, H. Shigesawa, and K. Takiyama, "Submillimeter guided-wave experiments with polyethylene slabe waveguides," presented at the *Fourth Int. Conf. Infrared and Millimeter Waves and their Applications*, (Miami Beach, FA), F-1-2, Dec. 1979.

[18] G. W. Chantry, J. W. Fleming, P. M. Smith, M. Cudby, and H. A. Willis, "Far infrared and millimeter-wave absorption spectra of some low-loss polymers," *Chem. Phys. Lett.*, vol. 10, pp. 473–477, Aug. 1971.

[19] E. S. Cassesdy and M. Cohn, "On the existence of leaky waves due to a line source above a grounded dielectric slab," *IRE Trans. Microwave Theory Tech.*, vol. MTT-9, pp. 243–247, May 1961.

[20] K. Solbach, "Electric probe measurements on dielectric image lines in the frequency range of 26–90 GHz," *IEEE Trans. Microwave Theory Tech.*, vol. MTT-26, pp. 755–758, Oct. 1978.

[21] S. Ayers, G. J. Davies, J. Haigh, D. Marr, and A. E. Parker, "Low-loss dielectric for 10-3000 GHz," *Proc. Inst. Elec. Eng.*, vol. 121, pp. 1447–1450, Nov. 1974.

[22] I. Tsujimoto, "Submillimeter-wave dielectric measurements using an open resonator," M.S. thesis, Doshisha University, Kyoto, Japan, 1981.

Millimeter Wavelength Frequency Multipliers

JOHN W. ARCHER

Abstract— **Mechanically tuneable millimeter wavelength frequency doublers typically exhibiting 10-percent conversion efficiency at any output frequency in the range 100–260 GHz have been fabricated. Output power varies from 10 mW at 100 GHz to 6 mW at 260 GHz, with a fixed tuned instantaneous 1-dB bandwidth typically 5 percent of the center frequency. A frequency tripler to 215-GHz output frequency is also described. For this device, a mechanically tuneable 3-dB bandwidth of 210 to 240 GHz was obtained, with a peak conversion efficiency of 6 percent at 4.8-mW output power.**

Manuscript received September 25, 1980; revised December 23, 1980. The National Radio Astronomy Observatory is operated by Associated Universities, Incorporated, under contract with the National Science Foundation.

The author is with the National Radio Astronomy Observatory, Charlottesville, VA 22903.

I. Introduction

SOURCES of millimeter wavelength power for heterodyne receiver local oscillator applications at wavelengths shorter than 3 mm have conventionally been expensive, short-lived klystrons. An alternate approach is to use efficient, broad-band frequency multipliers in conjunction with more reliable, lower frequency oscillators to provide power in the frequency range 100 GHz and above.